

6.6 Smoothing and Sharpening (Original images...)



FIGURE 6.39 HSI components of the RGB color image in Fig. 6.38(a). (a) Hue. (b) Saturation. (c) Intensity.

6.6.1 Colour Image Smoothing

Smoothing by neighbourhood averaging can be performed using RGB colour vectors,

$$\bar{\mathbf{c}}(x, y) = \frac{1}{K} \sum_{(x,y) \in S_{xy}} \mathbf{c}(x, y)$$

or can be carried out on a per-colour-plane basis

$$\bar{\mathbf{c}}(x, y) = \begin{pmatrix} \frac{1}{K} \sum_{(x,y) \in S_{xy}} R(x, y) \\ \frac{1}{K} \sum_{(x,y) \in S_{xy}} G(x, y) \\ \frac{1}{K} \sum_{(x,y) \in S_{xy}} B(x, y) \end{pmatrix}$$

Example 6.12:

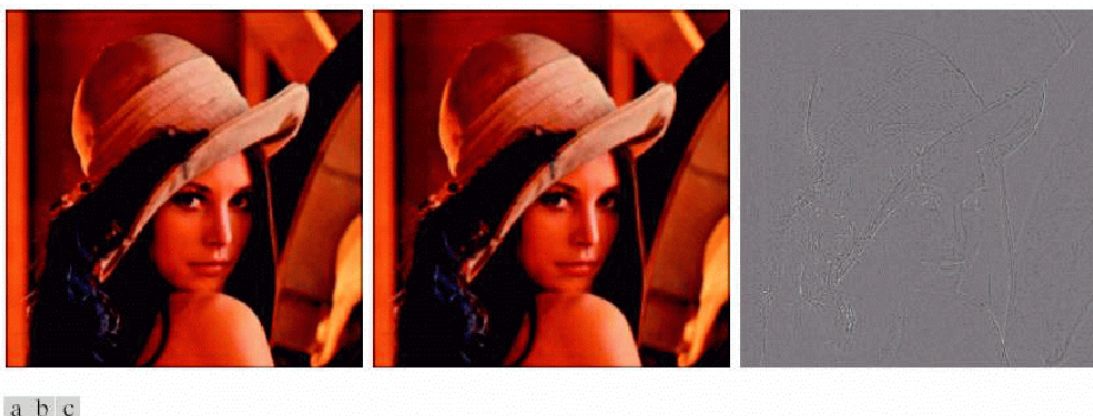


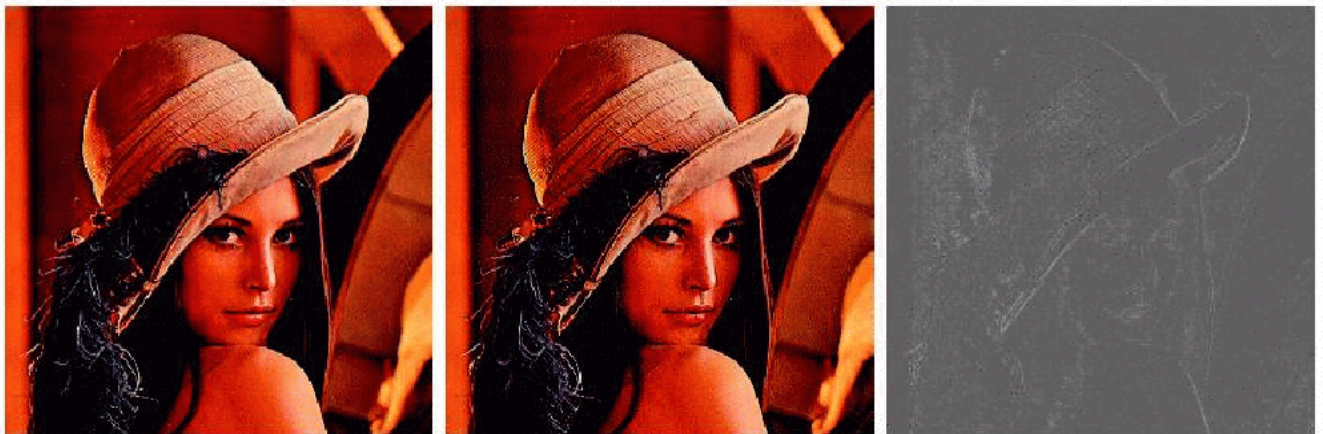
FIGURE 6.40 Image smoothing with a 5×5 averaging mask. (a) Result of processing each RGB component image. (b) Result of processing the intensity component of the HSI image and converting to RGB. (c) Difference between the two results.

6.6.2 Colour Image Sharpening

Similar to image smoothing, image sharpening can also be performed on a per-colour-plane basis (using the Laplacian),

$$\nabla^2[\mathbf{c}(x, y)] = \begin{pmatrix} \nabla^2 R(x, y) \\ \nabla^2 G(x, y) \\ \nabla^2 B(x, y) \end{pmatrix}$$

Example 6.13:

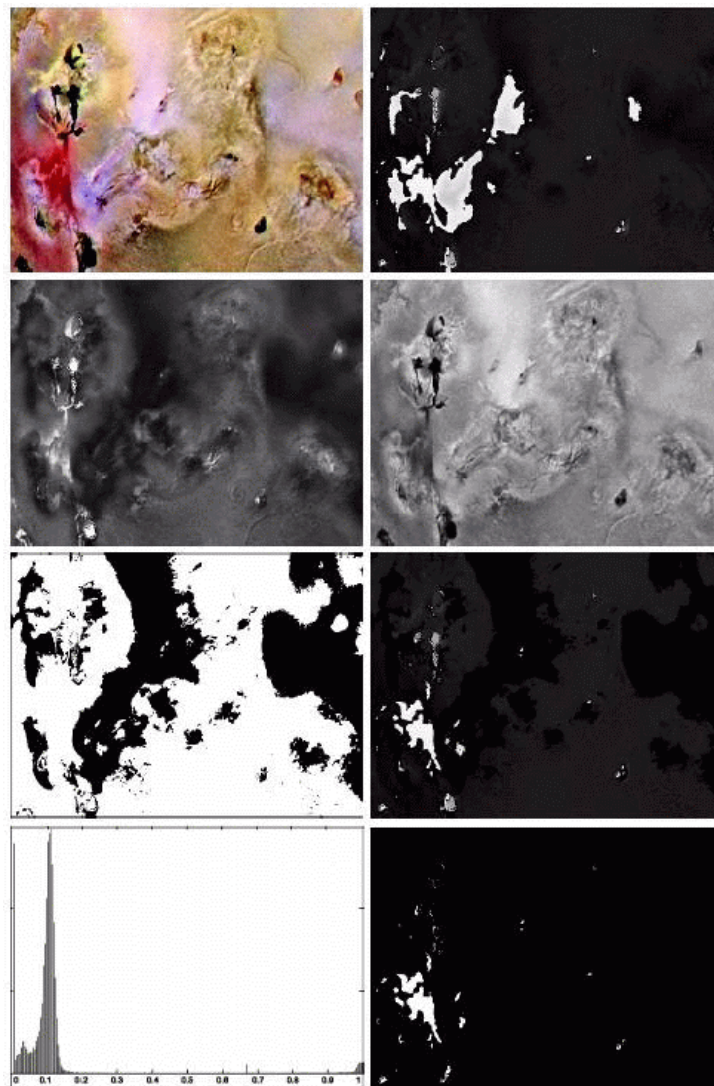


a b c

FIGURE 6.41 Image sharpening with the Laplacian. (a) Result of processing each RGB channel. (b) Result of processing the intensity component and converting to RGB. (c) Difference between the two results.

6.7 Colour Segmentation

6.7.1 Segmentation in HSI Colour Space Example 6.14



a b
c d
e f
g h

FIGURE 6.42 Image segmentation in HSI space. (a) Original. (b) Hue. (c) Saturation. (d) Intensity. (e) Binary saturation mask (black = 0). (f) Product of (b) and (e). (g) Histogram of (f). (h) Segmentation of red components in (a).

6.7.2 Segmentation in RGB Vector Space

Given a set of representative colour points, calculate average colour (\mathbf{a}) and (if necessary) covariance matrix (\mathbf{C})

Let \mathbf{z} denote an arbitrary point in RGB space

Three similarity measures:

(1) Euclidean distance

$$\begin{aligned} D(\mathbf{z}, \mathbf{a}) &= \|\mathbf{z} - \mathbf{a}\| \\ &= [(\mathbf{z} - \mathbf{a})^T (\mathbf{z} - \mathbf{a})]^{\frac{1}{2}} \\ &= [(z_R - a_R)^2 + (z_G - a_G)^2 + (z_B - a_B)^2]^{\frac{1}{2}} \end{aligned}$$

$D(\mathbf{z}, \mathbf{a}) \leq D_0 \Rightarrow$ points within solid spherical region

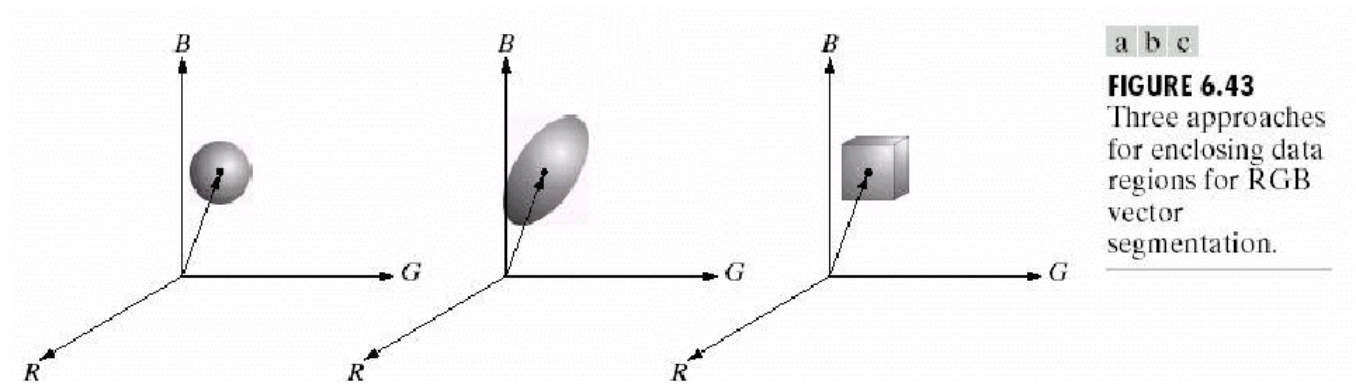
(2) “Mahalanobis”-like distance

$$D(\mathbf{z}, \mathbf{a}) = [(\mathbf{z} - \mathbf{a})^T \mathbf{C}^{-1} (\mathbf{z} - \mathbf{a})]^{\frac{1}{2}}$$

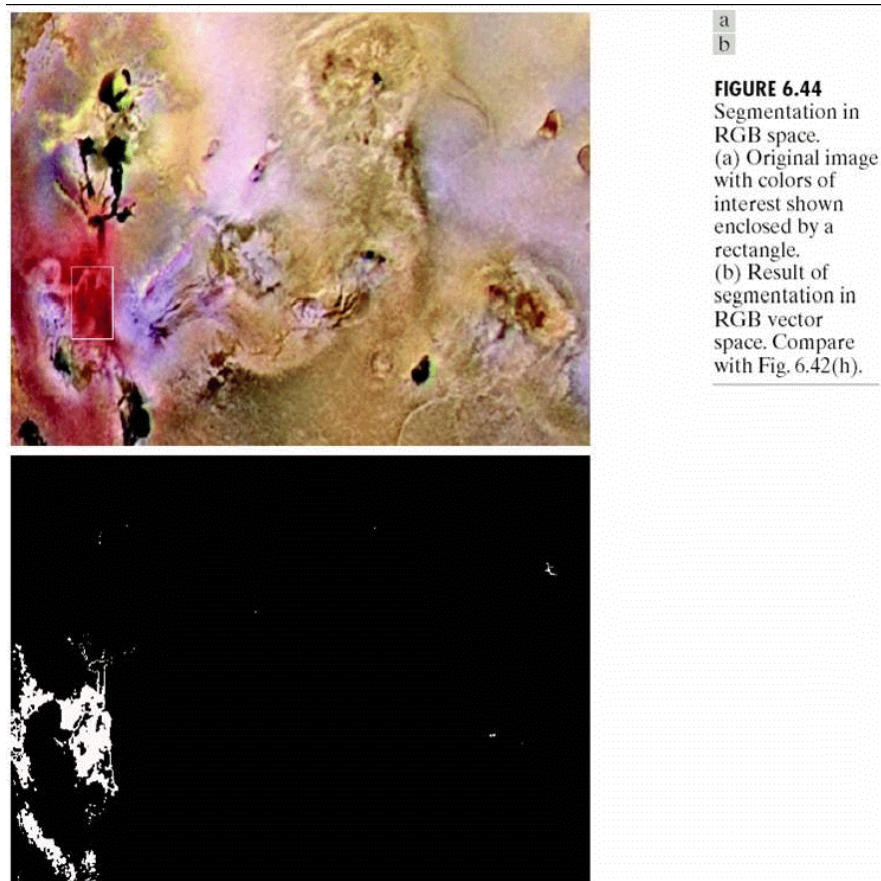
$D(\mathbf{z}, \mathbf{a}) \leq D_0 \Rightarrow$ points within solid ellipsoidal region

(3) Bounding box (computationally less expensive)

Centered at \mathbf{a} , dimensions proportional to standard deviations ($\sigma_R, \sigma_G, \sigma_B$) along colour axes

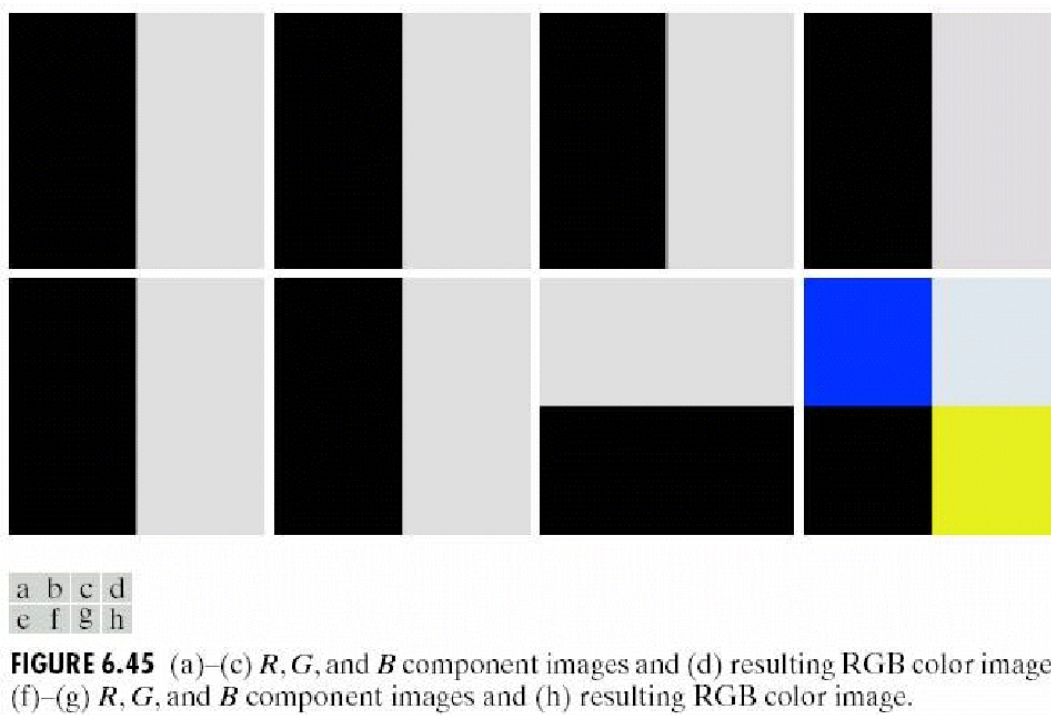


Example 6.15: Colour image segmentation in RGB space



6.7.3 Colour edge detection

Computing the gradient on individual (R,G,B) images (e.g. Sobel operators) and then using the results to form a colour image lead to erroneous results! Example...



Only consider gradient in middle of images. When we calculate gradient of respective component images and add results to form two RGB gradient images, the value of RGB gradient (in middle) is the same. This is clearly not the case here!

Edge detection in vector (e.g. RGB) space

Sobel operators can not be used. Di Zenzo's method:

$$\mathbf{u} = \frac{\partial R}{\partial x} \mathbf{r} + \frac{\partial G}{\partial x} \mathbf{g} + \frac{\partial B}{\partial x} \mathbf{b}, \quad \mathbf{v} = \frac{\partial R}{\partial y} \mathbf{r} + \frac{\partial G}{\partial y} \mathbf{g} + \frac{\partial B}{\partial y} \mathbf{b}$$

$$g_{xx} = \mathbf{u} \cdot \mathbf{u} = \mathbf{u}^T \mathbf{u} = \left| \frac{\partial R}{\partial x} \right|^2 + \left| \frac{\partial G}{\partial x} \right|^2 + \left| \frac{\partial B}{\partial x} \right|^2$$

$$g_{yy} = \mathbf{v} \cdot \mathbf{v} = \mathbf{v}^T \mathbf{v} = \left| \frac{\partial R}{\partial y} \right|^2 + \left| \frac{\partial G}{\partial y} \right|^2 + \left| \frac{\partial B}{\partial y} \right|^2$$

$$g_{xy} = \mathbf{u} \cdot \mathbf{v} = \mathbf{u}^T \mathbf{v} = \frac{\partial R}{\partial x} \frac{\partial R}{\partial y} + \frac{\partial G}{\partial x} \frac{\partial G}{\partial y} + \frac{\partial B}{\partial x} \frac{\partial B}{\partial y}$$

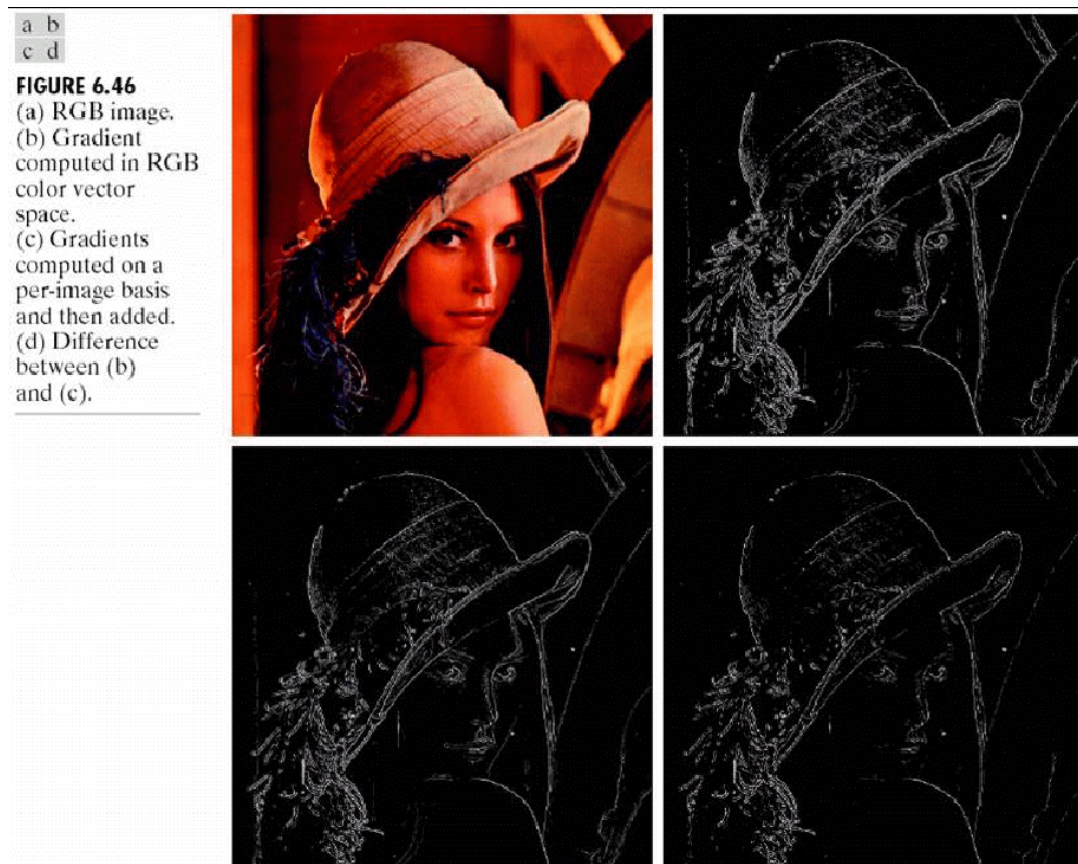
Direction of maximum rate of change of $\mathbf{c}(x, y)$:

$$\theta = \frac{1}{2} \tan^{-1} \left\{ \frac{2 g_{xy}}{(g_{xx} - g_{yy})} \right\}$$

Value of rate of change at (x, y) in direction of θ :

$$F(\theta) = \left\{ \frac{1}{2} [(g_{xx} + g_{yy}) + (g_{xx} - g_{yy}) \cos(2\theta) + 2g_{xy} \sin(2\theta)] \right\}^{\frac{1}{2}}$$

Example 6.16: Edge detection in vector (RGB) space



6.8 Noise in Colour Images

The noise content usually has the same characteristics in each colour channel, but channels can be affected differently when, e.g., the electronics of a particular channel malfunctions

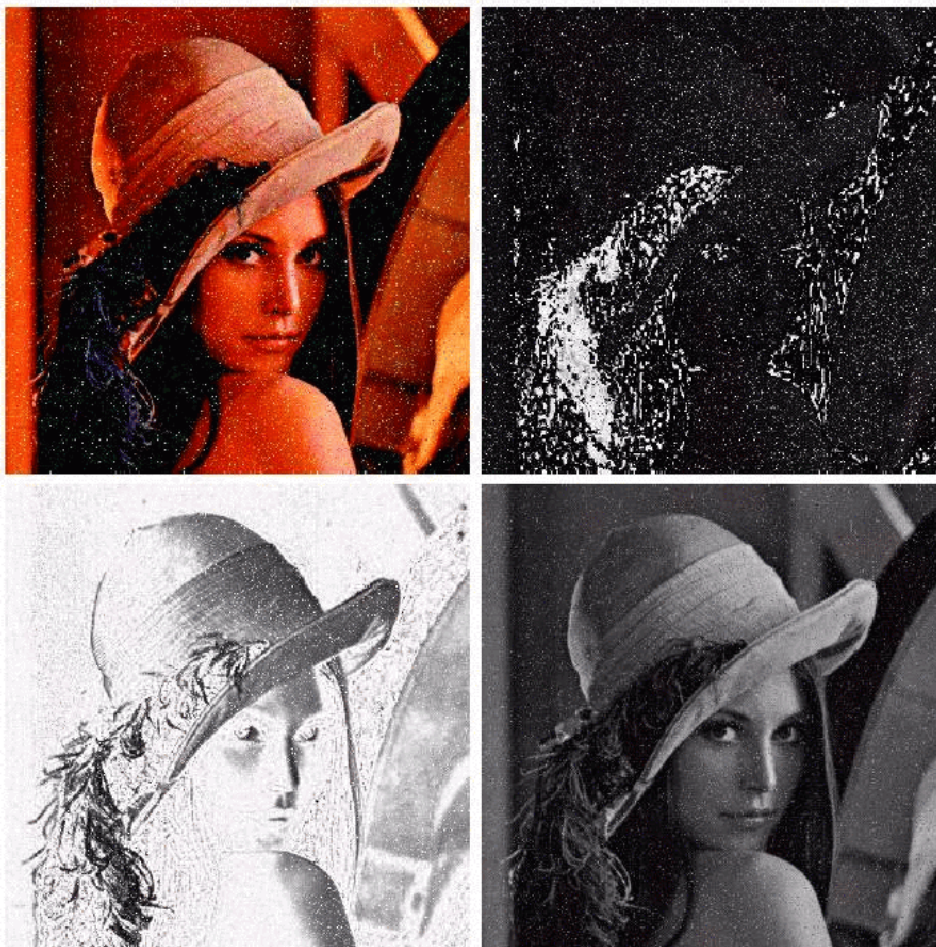
Example 6.17: Converting noisy RGB images to HSI





a b c

FIGURE 6.49 HSI components of the noisy color image in Fig. 6.48(d). (a) Hue. (b) Saturation. (c) Intensity.



a b
c d

FIGURE 6.50
(a) RGB image with green plane corrupted by salt-and-pepper noise.
(b) Hue component of HSI image.
(c) Saturation component.
(d) Intensity component.

Noise reduction using an averaging filter (linear) gives the same results in vector space as it does if the component images are processed independently. This is not the case for other filters, e.g. order statistics filters (vector ordering is beyond the scope of this course)

6.9 Colour Image Compression

Example 6.18: JPEG 2000 compression ($C_R = 230 : 1$)



a b
c d

FIGURE 6.51
Color image
compression.
(a) Original RGB
image. (b) Result
of compressing
and
decompressing
the image in (a).